(JNASR) Journal of Natural and Applied Sciences Research
Aigbekaen and Omorogbe, (2025). 1(1): 103-112. Available online at https://www.jnasr.iuokada.edu.ng. jnasr@iuokada.edu.ng

Mechanical, Electronic, Vibrational, Structural, and Thermodynamic Properties of ZrNiX (X-Pb, Sn) Half-Heusler alloys.

'Aigbekaen, E. E. and [2] Omorogbe, O. H.

'Department of Physics, Igbinedion University, Okada, Edo State, Nigeria

[2] *Department of Computer Science & Information Technology/Cyber Security, Igbinedion University, Okada, Edo State, Nigeria*

Corresponding Author:

Aigbekaen, E E

Department of Physics, College of Natural and Applied Sciences, Igbinedion University, Okada.

aigbekaen.eddy@iuokada.edu.ng. Tel.: 08053311659

Abstract

The mechanical, electrical, structural, vibrational, and thermodynamic properties of ZrNiX (X-Pb, Sn) half-Heusler alloys have all been considered using the first principle approach. We establish that the characteristics of the two alloys are comparable. Their phonon dispersion curve indicates phonon-phonon scattering, which suggests that they are good thermoelectric materials. It is discovered that both alloys exhibit thermodynamic and mechanical stability.

Keyword: Half Heusler alloys, Thermoelectric, Thermodynamics, Electronic Band structure, mechanical.

Introduction

Half-Heusler (HH) alloys have a wide range of intriguing physical features that make them one of the most attractive prospects for usage in spintronics, topological insulators, optoelectronic, photovoltaic, and thermoelectric applications (Moodera, 1995; Kämmerer, 2003; and Prinz, 1999). These alloys are used primarily because of their good mechanical, structural, electrical, and thermodynamic stability (Culp *et al.*, 2008; Wang, 2009; Yu *et al*., 2009; Kimura, 2010 and Wang, 2016). Investigating sustainable and effective materials in the half Heusler family that can turn waste heat into power is one way to prudently address the fast depletion of fossil fuels and their effects on the environment (Bhat e*t al*., 2015). The design of thermoelectric (TE) materials has successfully replaced degenerate semiconductors, which are made up of heavy, toxic, and scarce tellurium and lead elements, with inexpensive, non-toxic half-Heusler compound elements (such as nickel, tin, etc.) because their properties are similar to those of the TE materials that are currently on the market (Xia *et al*., 2000; Wu *et al*., 2007; and Muta *et al*.,2009) . Many studies of half-Heusler compounds with 18-valence electrons have resulted from the discovery of 54 thermodynamically stable half-Heuslers out of 400 that were not previously reported by Gautier and his coworkers (Gautier *et al*., 2015). It has been observed that certain half-Heusler compounds, such as (Ti, Zr, Hf)NiSn and (Ti, Zr, Hf)CoSb, have a comparatively high figure of merit (ZT values), a high power factor, and average thermal stability in both n- and p-type materials (Jung *et al*., 2010). Although these recently created narrow-gaped semiconductors' poor heat conductivity has restricted

their range of applications, numerous attempts have been undertaken to remedy the drop in thermal conductivity, with notable documented success (He *et al*., 2014; Jie *et al*.,2013; Lim *et al*., 2016; Caillat *et al*., 1997 and Dresselhaus *et al*., 2007). The aforementioned indicates that within the past 25 years, there has been an increase in interest in half-Heuslers and their general characteristics, including their mechanical, structural, thermodynamic, electronic, and lattice dynamics. Both theoretically (Guo, 2016) and empirically (Kurosaki *et al*., 2010), the relationships between the thermoelectric characteristics and the electronic structure and thermodynamic stability have been examined. Certain half-Heusler alloys' lattice thermal conductivities were shown to be in good agreement with experimental values using first principle calculations (Muta *et al*., 2009). Two distinct thermal analysis approaches have also been used to evaluate the thermal expansion and melting temperature of MNiSn type half-Heusler alloys in order to provide data that can be compared for TE industry (Kurosaki *et al*., 2010). Using antisite flaws, Qiu *et al*., 2010, performed an ab-initio simulation to investigate the band structure of MNISn. In order to determine the parameters employed in the prediction of lattice thermal conductivity, the effect of adding alloying metals such as extra nickel was investigated. The electronic structure, lattice dynamics, elastic, and thermoelectric properties of ZrNiPb were examined by Wang *et al*., 2016. They then used first principle calculations to dope with hafnium, which allowed them to examine the doping effect and propose new candidates for high performance thermoelectric materials, such as Zr_x Hf_{1-x} NiPb in both p- and n-type. Although various authors have attempted to address the lattice dynamics, mechanical, electronic, thermodynamic, and elastic properties of these HH alloys in different ways, no single paper has addressed all of the aforementioned properties, as well as the relationship between the thermal conductivity and figure of merit, which are the most crucial material properties for an effective TE material. In order to compare the two HH alloys and recommend the best suitable material for the creation of high performance TE devices, we examined the lattice dynamics, mechanical, electrical, elastic, and thermodynamic properties of ZrNi(Pb, Sn).

Methodology

The lattice dynamics of ZrNiX(Pb,Sn) have been calculated using first-principles methods. The density functional theory (DFT) utilizing the generalized gradient approximation, as executed in the Quantum Espresso software (Giannozzi *et al*., 2003), is employed. The projected augmented wave (PAW) approach is employed to formulate the potentials. The convergence test is initially conducted using a plane wave basis set with kinetic energy cut-offs of 952 eV for ZrNiPb and 816 eV for ZrNiSn. Monkhorst Pack meshes of 8x8x8 and 7x7x7 are utilized for the Brillouin zones of ZrNiPb and ZrNiSn, respectively. The final convergence test is conducted on the lattice constant, wherein the data file comprising strained lattice constants and their associated total energies for each alloy is fitted to the Birch-Murnaghan equation of state, resulting in the determination of the optimized lattice constant, bulk modulus, and pressure derivative. The mechanical and thermodynamic properties are calculated utilizing the thermocode (Dal Corso, 2016).

Table 1: The lattice constant a, bulk modulus B, the pressure derivative B' and the band gap of ZrNiX(X-Pb,Sn) including results from literature.

Compound	Ref	a(Å)	B(GPa)	B'(GPa)	E_g (eV)
ZrNiPb	Present	6.247	109.4	4.65	0.3937
	Literature	6.232	112.5	-	0.385[a] , 0.43[a]
ZrNiSn	Present	6.162	119.4	4.40	0.3937
	Literature	6.110	124.6	-	0.18[b] , 0.25[c]

[Wang *et al*., 2016][a] , [Rog *et al*., Grytsiv *et al*., 2016][b] , [Zou *et al*., 2013][c]

Table 2: The elastic constant C_{ij} , the Young modulus E, the shear modulus G all in GPa and the Poisson ration v, the bulk modulus-shear modulus ratio B/G, the average sound velocity and the Debye temperature of ZrNiX(X-Pb,Sn).

Compound	C_{11}	C_{12}	C_{44}	E	G	v	B/G	V_{ag} (m/s)	D_θ (K)
ZrNiPb	201.1	63.5	50.3	147.2	57.7	0.2758	1.8960	2691	293
Others	205.5	66.0	58.0	179.6	72.8	-	-	-	-
ZrNiSn	219.7	69.3	55.6	161.7	63.5	0.2743	1.8803	3188	353
Others	224.8[b]	74.7[b]	75.1[b]	187.7[b]	75.1[b]	0.2490[b]	1.66[b]	-	-

Results and discussion

Structural properties

A face-centered cubic structure with space group F-43m is the crystal structure of the 18-valence electron half-Heusler alloys. In our calculations, the Pb and Sn atoms are at Wyckoff positions 4b (1/2, 1/2,1/2), while the Zr and Ni atoms are at Wyckoff positions 4a (0,0,0) and 4c (1/4,1/4,1/4), respectively. During the convergence test, the lattice constants used in this work are determined. Fitting the strained lattice constants and their corresponding total energy to the Murnaghan equation of state yields the bulk modulus and the pressure derivative. Table 1 presents the results. Based on the bulk modulus, we found that ZrNiSn is more resistant to compressibility than ZrNiPb.

Electronic properties

The ZrNiX(X-Pb,Sn) electronic band structure and associated density of state (DOS) are displayed in Figures 1-4. Table 1 displays the band gap of the two alloys, indicating that they are low gap semiconductors. With their conduction band lowest at the high symmetry point X and their valence band maximum at the gamma point, these alloys are also indirect band gap semiconductors. The hybridization between the Zr-d, Ni-d, and Pb-p orbitals is demonstrated by the DOS of ZrNiPb shown in Fig. 3. The highest peak is found in the Ni-d orbital. Additionally, for ZrNiSn, the hybridization occurs (Aigbekaen and Ighrakpata, 2022) between the Zr-p, Ni-d, and Sn-p orbitals, with the Ni-d orbital exhibiting the largest peak. As seen in (Aigbekaen *et al*.,

2023; Iyorzor *et al*., 2021 and Okunzuwa and Aigbekaen, 2020), the DOS of both materials exhibits a strong increase in the valence band close to the Fermi energy, which is a sign of significant thermopower. In the ZrNiPb alloy, we found that the bond between Ni and Pb is greater than that between Ni and Zr, whereas in the ZrNiSn alloy, the binding between Ni and Sn is stronger than that between Ni and Zr.

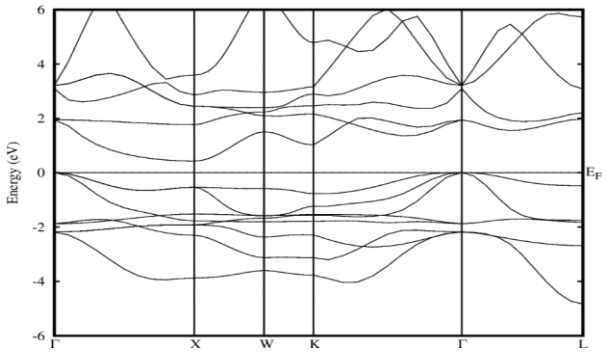

Fig1: The electronic band structure of ZrNiPb

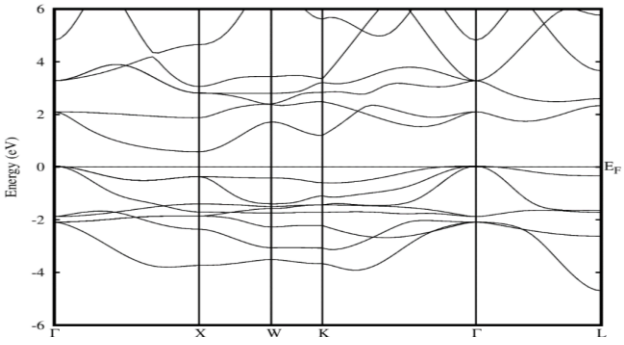

Fig2 : The electronic band structure of ZrNiSn

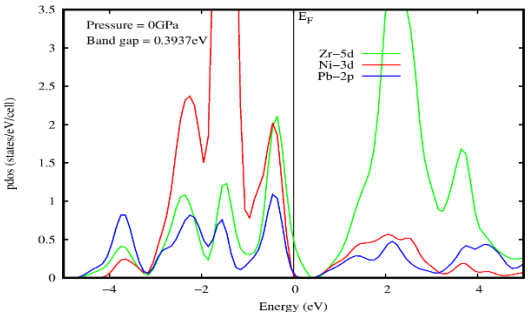

Fig3: Partial density of state of ZrNiPb

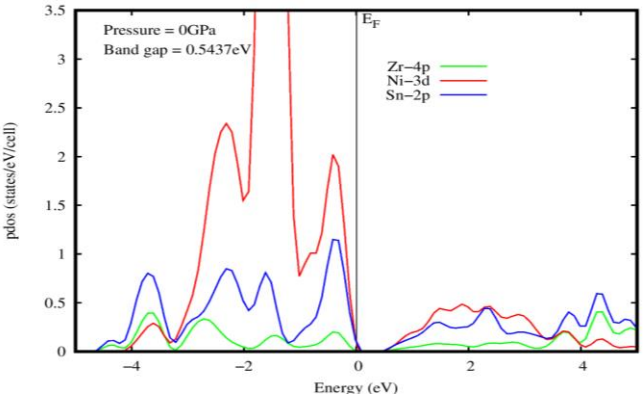

Fig4: Partial density of state of ZrNiSn

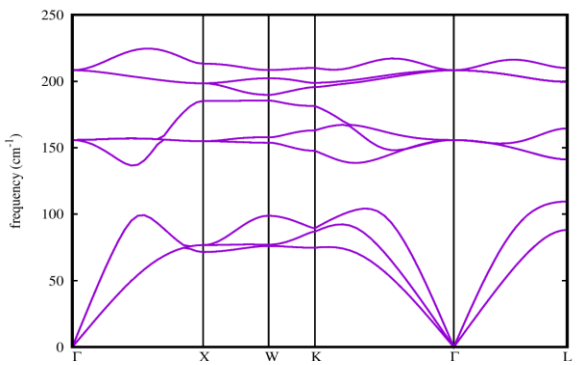

3.3. Lattice dynamics

Fig5: Phonon dispersion curve of ZrNiPb

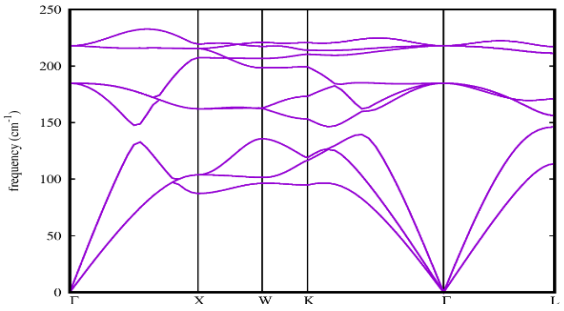

Fig6: Phonon dispersion curve of ZrNiSn

The ZrNiX (X=Pb,Sn) phonon dispersion curves, which provide information on the lattice dynamics of materials, have been calculated and are dynamically stable since the high symmetry points do not have any negative frequencies. These curves are displayed in Figs. 5 and 6. With three acoustic and six visual modes, Figs. 5 and 6 exhibit comparable phonon dispersion curves. We found that ZrNiPb exhibits a larger gap between the acoustic mode and the lower optical mode than ZrNiSn, indicating a stronger phonon-phonon scattering. Additionally, we observed from the phonon dispersion curves that the formal has a larger group velocity because the acoustic mode of ZrNiSn is more disseminated than that of ZrNIPb at higher frequencies. Low thermal conductivity is indicated by this phonon-phonon scattering, particularly in bulk semiconductors (Gudelli *et al.*, 2015 and Zou *et al.*, 2013).

Mechanical Properties

ZrNiPb and ZrNiSn mechanical characteristics have been calculated and are shown in Table 2. Since the alloys crystallize in a cubic form, the mechanical parameters include, Poisson ratio, shear modulus, and elastic constants C_{11}, C_{12}, and C_{44}. When it comes to determining the mechanical stability of solid materials and the forces keeping them together, the elastic constants are crucial. According to equation 1, both alloys meet the requirements for mechanical stability.

$C_{11} > 0$, $(C_{11}+2C_{12}) > 0$, $C_{44}>0$, and $C_{11}>C_{12}$. (1)

The Voigt-Reuss-Hill approximation is used to compute the young modulus and the shear modulus, which demonstrate how resistant these alloys can be to volume and shear deformation. Table 2 makes it evident that ZrNiSn is more difficult than ZrNiPb. Both materials are brittle according to the B/G ratio since their B/G ratios exceed 1.75.

Thermodynamic properties

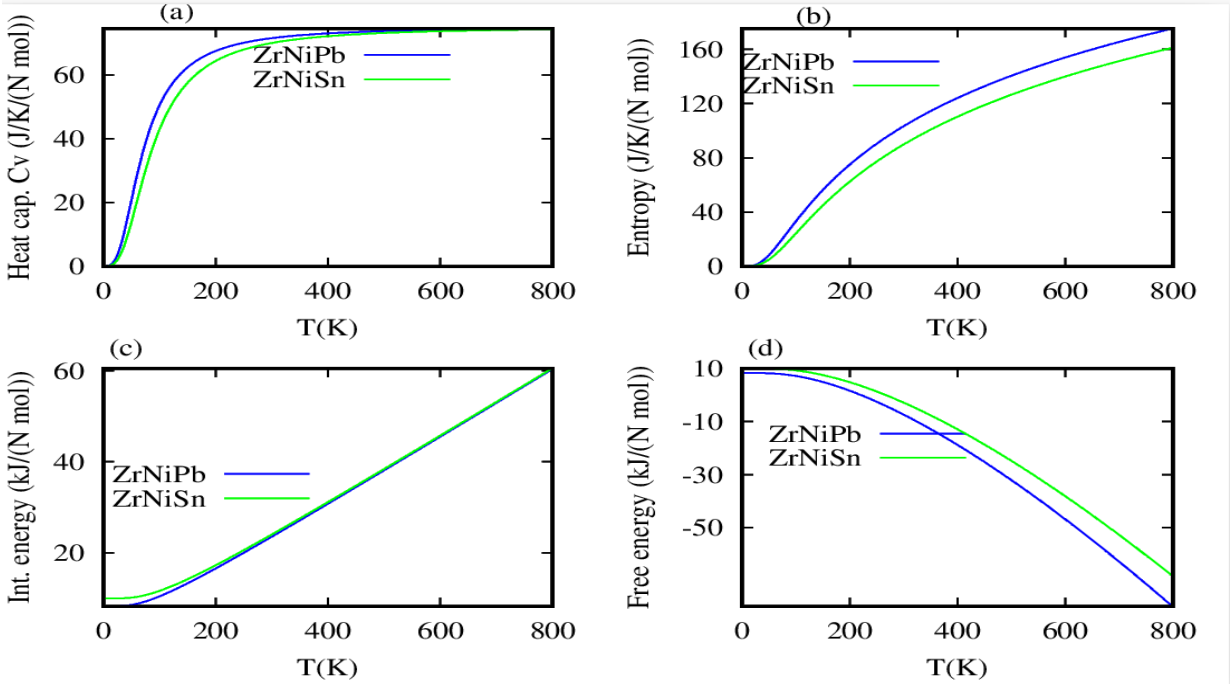

Fig7: Thermodynamic properties of ZrNiX(X=Pb, Sn), (a) the specific heat capacity at constant volume. (b) the entropy, (c) the internal, and (d) the free energy.

The internal energy, Gibb's free energy, entropy, specific heat capacity at constant volume, and Debye temperature, melting temperature, and average sound velocity of the two alloys have all been calculated and are displayed in Fig. 7. As we can see from Fig. 7a, the specific heat capacities of the two alloys comply with the Dulong-Petit rule at high temperatures and the T_3 law at low temperatures. Both alloys' curves for the other thermodynamic parameters are comparable and meet the requirements of thermodynamics. ZrNiPb and ZrNiSn have zero point energies of 8.2358 kJ/Nmol and 9.86452 kJ/Nmol, respectively. We observed that at high temperatures, the two alloys' specific heat capacities and internal energies converge. We also used equation (2) (Fine *et al*., 1984).

T_m = (607+9.3B±300)K

where B is the bulk modulus, to calculate the theoretical melting temperatures of both alloys, which came out to be 1347K for ZrNiPb and 1429K for ZrNiSn, respectively.

Conclusion

The electrical, structural, mechanical, vibrational, and thermodynamic properties of ZrNiX (X=Pb, Sn) have been calculated from first principles. We establish that each of these alloys exhibit thermodynamic and mechanical stability. It is mentioned how the phonon dispersion curve, the electronic band structure, and the thermoelectric properties are related.

REFERENCES

Aigbekaen, E.E., and Ighrakpata, F. C. (2022): The First Principal Study Of The Structural, Electronic, Elastic, Vibrational And Thermal Properties Of Cscl Type-Ercu Alloy. AAN Journal of

Sciences, Engineering & Technology Vol. 1, Issue 1, pp. 1-11.

Aigbekaen, E.E., Okei, J., and Ighrakpata, F.C. (2023): First-Principles Study: Some Physical Properties of Half-Heusler Alloys XCrBi (X=Hf, Ti, and Zr). Journal of Science and Technology Research 5(4), 118-127.

Bhat, I.H., Yousuf, S., Bhat, T.M. and Gupta, D.C. (2015): Investigation of electronic structure, magnetic and transport properties of half-metallic Mn2CuSi and Mn2ZnSi Heusler alloys. Journal of Magnetism and Magnetic Materials, 395, pp.81-88.

Caillat, T., Fleurial, J.P. and Borshchevsky, A. (1997): Preparation and thermoelectric properties of semiconducting Zn4Sb3. Journal of Physics and Chemistry of Solids, 58(7), pp.1119-1125.

Culp, S.R., Simonson, J. W., Poon, S.J., Ponnambalam, V., Edwards, J. and Tritt, T.M. (2008): (Zr, Hf) Co (Sb, Sn) half-Heusler phases as high-temperature (> 700° C) p-type thermoelectric materials. Applied Physics Letters, 93(2), p.022105.

Dal Corso, A. (2016); Elastic constants of beryllium: a first-principles investigation. Journal of Physics: Condensed Matter, 28(7), p.075401.

Dresselhaus, M.S., MS Dresselhaus, G. Chen, MY Tang, RG Yang, H. Lee, DZ Wang, ZF Ren, J.-P. Fleurial, and P. Gogna (2007): New Directions for Low-Dimensional Thermoelectric Materials Adv. Mater. 19, 1043. Adv. Mater., 19, p.1043.

Fine, M.E., Brown, L.D. and Marcus, H.L. (1984): Elastic constants versus melting temperature in metals. Scriptametallurgica, 18(9), pp.951-956.

Gautier, R., Zhang, X., Hu, L., Yu, L., Lin, Y., Sunde, T.O., Chon, D., Poeppelmeier, K.R. and Zunger, A. (2015): Prediction and accelerated laboratory discovery of previously unknown 18-electron ABX compounds. Nature chemistry, 7(4), p.308.

Giannozzi, P., Baroni, S., Bonini, N., Calandra, M., Car, R., Cavazzoni, C., Ceresoli, D., Chiarotti, G.L., Cococcioni, M., Dabo, I. and Dal Corso, A. (2009): QUANTUM ESPRESSO: a modular and open-source software project for quantum simulations of materials. Journal of physics: Condensed matter, 21(39), p.395502.

Gudelli, V.K., Kanchana, V., Vaitheeswaran, G., Singh, D.J., Svane, A., Christensen, N.E. and Mahanti, S.D. (2015): Electronic structure, transport, and phonons of SrAg Ch F (Ch= S, Se, Te): Bulk superlatticethermoelectrics. Physical Review B, 92(4), p.045206.

Guo, S.D. (2016): Thermoelectric properties of half-Heusler ZrNiPb by using first principles calculations. RSC Advances, 6(53), pp.47953-47958.

He, R., Kim, H.S., Lan, Y., Wang, D., Chen, S. and Ren, Z. (2014): Investigating the thermoelectric properties of p-type half-HeuslerHf x (ZrTi) 1 x CoSb 0.8 Sn 0.2 by reducing Hf concentration for power generation. Rsc Advances, 4(110), pp.64711-64716.

Iyorzor,B.E., Babalola, M.I., and Aigbekaen,E.E. (2018): Ab initio Calculation of the Structural,

Mechanical and Thermodynamic Properties of Beryllium Sulphides, BeS, J.Appl.Sci.Environ.Manage.,Vol.22(1), 41-46.

Jie, Q., Wang, H., Liu, W., Wang, H., Chen, G. and Ren, Z. (2013): Fast phase formation of double-filled p-type skutterudites by ball-milling and hot-pressing. Physical Chemistry Chemical Physics, 15(18), pp.6809-6816.

Jung, D.Y., Kurosaki, K., Kim, C.E., Muta, H. and Yamanaka, S. (2010): Thermal expansion and melting temperature of the half-Heusler compounds: MNiSn (M= Ti, Zr, Hf). Journal of Alloys and Compounds, 489(2), pp.328-331.

Kämmerer, S., Heitmann, S., Meyners, D., Sudfeld, D., Thomas, A., Hütten, A. and Reiss, G. (2003): Room-temperature preparation and magnetic behavior of Co 2 MnSi thin films. Journal of applied physics, 93(10), pp.7945-7947.

Lim, Y.S., Park, K.H., Tak, J.Y., Lee, S., Seo, W.S., Park, C.H., Kim, T.H., Park, P., Kim, I.H. and Yang, J. (2016): Colligative thermoelectric transport properties in n-type filled CoSb3 determined by guest electrons in a host lattice. Journal of Applied Physics, 119(11), p.115104.

Moodera, J.S., Kinder, L.R., Wong, T.M. and Meservey, R. (1995): Large magnetoresistance at room temperature in ferromagnetic thin film tunnel junctions. Physical review letters, 74(16), p.3273.

Muta, H., Kanemitsu, T., Kurosaki, K. and Yamanaka, S. (2009): High-temperature thermoelectric properties of Nb-doped MNiSn (M= Ti, Zr) half-Heusler compound. Journal of Alloys and Compounds, 469(1-2), pp.50-55.

Okunzuwa, I. S., and Aigbekaen, E.E. (2021): Structural Optimization, Electronic Band Structure, Mechanical and Thermodynamics Properties of Fe3 Al. Physical Science International (JournalArticle no.PSIJ.67620) 25(2): 1-11.

Okunzuwa, S., and Aigbekaen, E. (2020): Structural Optimization and the Study of the Electronic, Mechanical, Thermodynamic and Phonon Properties of Mg2Sn from First Principle. Physical Science International (JournalArticle no.PSIJ.67620) 24(12): 60-71.

Prinz, G.A. (1999): Magnetoelectronics applications. Journal of magnetism and magnetic materials, 200(1-3), pp.57-68.

Qiu, P., Yang, J., Huang, X., Chen, X. and Chen, L.. (2010): Effect of antisite defects on band structure and thermoelectric performance of ZrNiSn half-Heusler alloys. Applied Physics Letters, 96(15), p.152105.

Rogl, G., Grytsiv, A., Gürth, M., Tavassoli, A., Ebner, C., Wünschek, A., Puchegger, S., Soprunyuk, V., Schranz, W., Bauer, E. and Müller, H. (2016): Mechanical properties of half- Heusler alloys. ActaMaterialia, 107, pp.178-195.

Wang, L.L., Miao, L., Wang, Z.Y., Wei, W., Xiong, R., Liu, H.J., Shi, J. and Tang, X.F. (2009): Thermoelectric performance of half-Heusler compounds TiNiSn and TiCoSb. Journal of Applied Physics, 105(1), p.013709.

Wang. D, Wang, G and Li, W (2016): First Principle study of elastic, electronic and thermoelectric properties of Phys. Lett. A 1-7, 24149.

Wu, T., Jiang, W., Li, X., Zhou, Y. and Chen, L. (2007): Thermoelectric properties of p-type Fe-doped TiCoSb half-Heusler compounds. Journal of Applied Physics, 102(10), p.103705. [12] Sekimoto, T., Kurosaki, K., Muta, H. and Yamanaka, S., 2007. High-thermoelectric figure of merit realized in p-type half-Heusler compounds: ZrCoSnxSb1-x. Japanese Journal of Applied Physics, 46(7L), p.L673.

Xia, Y., Bhattacharya, S., Ponnambalam, V., Pope, A.L., Poon, S.J. and Tritt, T.M. (2000): Thermoelectric properties of semimetallic (Zr, Hf) CoSb half-Heusler phases. Journal of applied physics, 88(4), pp.1952-1955.

Zou, D.F., Xie, S.H., Liu, Y.Y., Lin, J.G. and Li, J.Y. (2013): Electronic structure and thermoelectric properties of half-Heusler Zr0. 5HfO. 5NiSn by first-principles calculations. Journal of Applied Physics, 113(19), p.193705.